

AD-A041 959

RCA LABS PRINCETON N J
BASIC ADHESION MECHANISMS IN THICK AND THIN FILMS.(U)
APR 77 T T HITCH, K R BUBE

F/G 11/1

N00019-77-C-0176

UNCLASSIFIED

PRRL-77-CR-18

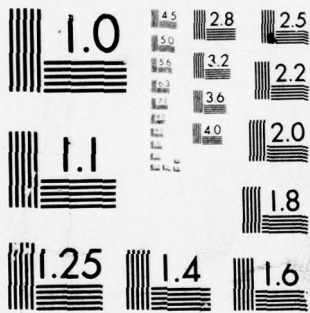
NL

| OF |
AD
A041 959



END

DATE
FILMED
8-77



MICROCOPY RESOLUTION TEST CHART
NATIONAL BUREAU OF STANDARDS-1963-A

ADA041959



UNCLASSIFIED

SECURITY CLASSIFICATION OF THIS PAGE (When Data Entered)

REPORT DOCUMENTATION PAGE		READ INSTRUCTIONS BEFORE COMPLETING FORM
1. REPORT NUMBER	2. GOVT ACCESSION NO.	3. RECIPIENT'S CATALOG NUMBER
4. TITLE (and Subtitle)		5. TYPE OF REPORT & PERIOD COVERED
6. BASIC ADHESION MECHANISMS IN THICK AND THIN FILMS.		Quarterly Report, No. 1, (1-1-77 to 3-31-77)
7. AUTHOR(s)		6. PERFORMING ORG. REPORT NUMBER
Thomas T. Hitch and Kenneth R. Bube		PRRL-77-CR-18 1 Jan - 31 Mar 77
9. PERFORMING ORGANIZATION NAME AND ADDRESS		8. CONTRACT OR GRANT NUMBER(s)
RCA Laboratories Princeton, New Jersey 08540		NO0019-77-C-0176 new
11. CONTROLLING OFFICE NAME AND ADDRESS		12. REPORT DATE
Naval Air Systems Command Washington, DC 20361		30 Apr 1977
14. MONITORING AGENCY NAME & ADDRESS (if different from Controlling Office)		13. NUMBER OF PAGES
(12) 29p.		29
		15. SECURITY CLASS. (of this report)
		15a. DECLASSIFICATION/DOWNGRADING SCHEDULE
		N/A
16. DISTRIBUTION STATEMENT (of this Report)		
APPROVED FOR PUBLIC RELEASE: DISTRIBUTION UNLIMITED		
17. DISTRIBUTION STATEMENT (of the abstract entered in Block 20, if different from Report)		
18. SUPPLEMENTARY NOTES		
19. KEY WORDS (Continue on reverse side if necessary and identify by block number)		
Sintering theory Liquid-phase sintering Gold powder Reactive bonding Spinels		
20. ABSTRACT (Continue on reverse side if necessary and identify by block number)		
This is the first quarterly report of the fourth in a series of one-year contracts at RCA to study, in particular, the adhesion mechanisms in thick-film conductors. It states the objectives of this year's study plan and describes the way in which research is based on earlier results obtained at RCA; on work done by the Naval Research Laboratories and Purdue University, both of which participate with RCA		

DD FORM 1473
1 JAN 73

UNCLASSIFIED

SECURITY CLASSIFICATION OF THIS PAGE (When Data Entered)

299000 ✓

draft
page
1/1

UNCLASSIFIED

SECURITY CLASSIFICATION OF THIS PAGE (When Data Entered)

20.

in the NASC contract program entitled Basic Adhesion Mechanisms in Thick and Thin Films; and on other studies.

Study → The primary objective of this year's work on the program at RCA is to construct models that will characterize the development of thick-film conductor adhesion, so that film properties may be predicted from the physical and chemical nature of the ink and substrate materials and from the processing to which these materials are subjected.

The work of modeling the frit-bonded film adhesion strength has been divided into two parts: one is the development of the microstructure; the other is the description of the adhesion strength in terms of the microstructure, the metal-phase/binder-phase interfacial adhesion, and other material properties.

The study of reactively bonded and mixed-bonded inks seeks to model the formation of the binder-phase structure and to understand the behavior of that structure. This involves identification of the important structures and the study of the kinetics of their formation.

In this quarter's work with frit-bonded inks, physical measurements of the properties of a gold powder developed for this study were completed. Also, sintering theories applicable to thick-film conductors were examined, particularly with reference to liquid-phase-assisted densification processes. Data for metal and glass systems studied by RCA earlier in the contract series were examined for conformance with the theories considered most likely to apply.

In the study of mixed-bonded and reactively bonded conductors, x-ray diffraction of powder samples of the binder phases of several high-adhesion-strength gold- and silver-based conductor films indicated that the formation of a spinel phase was important to the adhesion mechanism in these materials. The spinel is hypothesized to have the form $\text{Mg}_x\text{Cu}_{1-x}\text{Al}_2\text{O}_4$.

UNCLASSIFIED

SECURITY CLASSIFICATION OF THIS PAGE (When Data Entered)

PREFACE

This quarterly report describes work performed in the Process and Applied Materials Research Laboratory of RCA Laboratories under Contract No. N00019-77-C-0176. Dr. Paul Rappaport is the Laboratory Director and Dr. George L. Schnable is the Project Supervisor and Group Head. Dr. Thomas T. Hitch is the Project Scientist and, with Kenneth R. Bube, comprises the principal research team. James Willis is the Government Project Monitor.

It is a pleasure to acknowledge the help of R. J. Paff, who has contributed to this study by his use of x-ray diffraction techniques for phase identification, and to B. Seabury for his work in scanning electron microscopy. We also acknowledge the able assistance of E. J. Conlon and A. C. Miller in the preparation of samples and in the day-to-day pursuit of this study. Discussions throughout the work with Dr. G. L. Schnable and his reviews of the manuscript were most valuable.

We acknowledge helpful discussions with a number of the scientists studying thick-film technology in several companies and government laboratories. Discussions with members of the Naval Research Laboratories team working in coordination with RCA, including Dr. Jim Murday, Dr. Paul Becher, and Dr. Bill Bascom; with the Project Monitor, Mr. James Willis; and with his supervisor, Dr. Herbert J. Mueller, have been particularly useful.

APPROVED BY	
RTIS	RTIS Section <input checked="" type="checkbox"/>
RTS	RTS Section <input type="checkbox"/>
TRANSMISSION IDENTIFICATION	
DISTRIBUTION/AVAILABILITY CODES	
Dist.	AVAIL. and/or SPECIAL
<input checked="" type="checkbox"/>	<input type="checkbox"/>

TABLE OF CONTENTS

Section	Page
I. INTRODUCTION	1
II. FRIT-BONDED INKS	3
A. Sintering Theories Relevant to Fritted Metallization	3
B. Powder Preparation	12
C. Isothermal Shrinkage	14
III. REACTIVELY BONDED AND MIXED-BONDED FILMS	16
IV. FUTURE WORK	21
REFERENCES	23

LIST OF ILLUSTRATIONS

Figure	Page
1. Neck growth during initial stage sintering	6
2. Typical metallization firing profile	6
3. Densification during liquid-phase sintering	8
4. Shrinkage via rearrangement and other processes vs volume fraction of liquid phase	8
5. Liquid bridge between particles and resultant force	9
6. MK-2 gold powder - as precipitated	13
7. MK-2 gold powder - sintered at 500°C for 2 min	13
8. Shrinkage of gold powders at 900°C	14
9. Shrinkage of gold powders plus 10 vol pct E1527 glass at 900°C . . .	15

SECTION I

INTRODUCTION

This is the first quarterly report on a contract which is the fourth in a series of one-year programs at RCA, sponsored by the Naval Air Systems Command. The object of the study series has been to improve the understanding of hybrid film materials and, particularly, of the property of adhesion strength in thick-film conductors.

In each of the first three years of study, investigation was confined principally to one or two new classes of conductor ink. Gold conductors were studied in 1974; copper and silver were added in 1975; and gold-platinum-type conductors were first studied in 1976.

In each of these studies a broad spectrum of commercial inks was chemically analyzed, printed, and fired with a matrix of processing variations; adhesion strength and other physical properties were then measured on the fired films. Analysis of the ink powder morphology, the bonding phase-to-metal phase interface microstructure in the fired films, and other data allowed classification into three classes: frit-bonded, reactively bonded, and mixed-bonded inks. These classifications relate ink chemistry to the behavior of adhesion strength as influenced particularly by firing temperature.

A second part of each of the contract studies investigated the fundamental properties of materials characteristic of those used in thick-film paste formulations. The wetting and spreading of glass on metal and ceramic surfaces, the sintering of metal powders with or without the presence of glass, and the measurement of the adhesion of the film prepared by innovative methods are only some of the properties that have been measured.

The achievements of the first three years of study have produced a broad base of data on thick-film conductors, their adhesion, and some of the processes important to their behavior. Although most data are more phenomenological than theoretical, several individual inks and certain model film materials have been described rather thoroughly. At RCA, as a result of these studies, the chemical constituents and some physical properties of the conductor pastes, model ink powders, and substrates have been classified and thus related to the adhesion strength. In addition, the theories of sintering and wetting, which are

pertinent to the development of film properties in thick-film conductors, have been examined. However, no attempt to predict the properties of ink materials has been attempted.

To test our understanding of thick-film conductor materials, it is desirable to formulate theories for their behavior, which will model the development of adhesion strength. During the firing of thick-film conductors a large number of reactions occur that could affect their adhesion. It is believed to be possible, however, to form a theory that emphasizes the effects of the most important reactions. Even though such a theory will doubtless require the use of adjustable parameters to model film behavior, such an approach can be highly informative and should improve our understanding of these materials.

Accordingly, a major objective of the fourth year in the study of "Basic Adhesion Mechanisms in Thick and Thin Films" is to create models of the development of adhesion strength properties in thick-film conductors and to test those models. The plan calls for the separation of the work into two major parts: first, the study of frit-bonded inks; second, the study of mixed-bonded inks and reactively bonded inks.

Because of the complexity of directly modeling adhesion strength on the basis of the ink characteristics alone, the study of frit-bonded inks will proceed in two steps. One is the development of film microstructure during processing. The other is the modeling of adhesion strength development as a function of the microstructure and of the surface energy between the metal and the binder phase.

The work on mixed-bonded and reactively bonded inks will similarly require treatment of strength versus microstructures and interfacial energies. In addition, however, for these materials the nature of the binder phase structures will also be studied. Both the identification of the binder phase and the kinetics of its development will be examined.

SECTION II

FRIT-BONDED INKS

A. SINTERING THEORIES RELEVANT TO FRITTED METALLIZATION

A recent review of sintering theories was published by Vest [1] in preparation for a discussion of models pertaining to thick-film resistors. The several theoretical mechanisms which, according to Vest, describe neck growth and shrinkage behavior, are tabulated in Tables 1 and 2, respectively. While the volumetric ratios of conductive and insulating phases differ considerably for thick-film resistors and metallizations, the basic mechanisms are still considered applicable. As shown in Fig. 1, the classical model of sintering phenomena is based on the approach of two spherical particles of radius, r , and growth of the neck radius, x . The relationship between the neck radius, x , and particle radius, r , after sintering isothermally at a temperature, T , for a time, t , can be expressed as

$$\left(\frac{x}{r}\right)^n = F(T) r^{-m} t \quad (1)$$

Appropriate values of $F(T)$, m , and n can be found in Table 1. Similarly, the shrinkage in powder compacts, $\Delta L/L_0$, where ΔL is the change in length, and L_0 the original length is also a function of temperature, particle radius, and time, viz.,

$$\frac{\Delta L}{L_0} = G(T) r^{n'} t^{m'} \quad (2)$$

The values for $G(T)$, m' , and n' are found in Table 2.

In frit-bearing metallizations, the frit becomes quite fluid with increasing temperature i.e., the viscosity decreases exponentially. A typical metallization firing profile is shown in Fig. 2. Under this firing profile, organic binders are burned between 100 and 400°C. As shown by Eqs. (1) and (2), neck growth and shrinkage are inversely related to particle size. Hence, at the

1. R. W. Vest, "Conduction Mechanisms in Thick-Film Microcircuits," Final Technical Report under ARPA Order No. 1642, Grant Nos. DAHC-15-70-G7 and DAHC-15-73-G8. Grantee: Purdue Research Foundation, Dec. 1975.

TABLE 1. SUMMARY OF NECK GROWTH RELATIONSHIPS [1]

<u>Mechanism</u>	<u>F(T)</u>	<u>n</u>	<u>m</u>
Newtonian Viscous Flow	$\frac{3}{2} \frac{\gamma_{SV}}{\eta}$	2	1
Volume Diffusion	$\frac{40\gamma_{SL}\delta_{\ell}^3 D_V}{KT}$	5	3
Surface Diffusion	$\frac{56\gamma_{SL}\delta_{\ell}^4 D_S}{KT}$	7	4
Grain-Boundary Diffusion	$\frac{96\gamma_{SL}\delta_o b D_g}{KT}$	6	4
Evaporation-Condensation	$\frac{3\pi M \alpha_1 P_o \gamma_{SL} (M/2\pi RT)^{\frac{1}{2}}}{d_1^2 RT}$	3	2
Solution-Precipitation:			
A. Kingery's Model	$\frac{48K_1 \delta C_o \gamma_{LV} V_o D}{K_2 RT}$	6	4
1. Diffusion-Controlled Process			
2. Reaction-Controlled Process	$\frac{8K_1 C_o \gamma_{LV} V_o K_T}{K_2 RT}$	4	2
B. Without Shrinkage	$\frac{3\pi M \alpha_1 C_o \gamma_{SL} (M/2\pi RT)^{\frac{1}{2}}}{d_1^2 RT}$	3	2

TABLE 2. SUMMARY OF SHRINKAGE RELATIONSHIPS [1]

<u>Mechanism</u>	<u>G(T)</u>	<u>n'</u>	<u>m'</u>
Newtonian Viscous Flow	$\frac{3}{4} \frac{\gamma_{SV}}{\eta}$	1	1
Volume Diffusion	$\frac{40 \gamma_{SL} \delta_{\ell}^3 D_V}{KT}$	$\frac{2}{5}$	$\frac{6}{5}$
Grain-Boundary Diffusion	$\frac{12 \gamma_{SL} \delta_o b D_g}{KT}$	$\frac{1}{3}$	$\frac{4}{3}$
Solution-Precipitation:			
Kingery's Model			
1. Diffusion-Controlled Process	$\frac{6 K_1 \delta C_o \gamma_{LV} V_o D}{K_2 RT}$	$\frac{1}{3}$	$\frac{4}{3}$
2. Reaction-Controlled Process	$\frac{2 K_1 C_o \gamma_{LV} V_o K_T}{K_2 RT}$	$\frac{1}{2}$	1

LEGEND FOR EQUATIONS IN TABLES 1 AND 2

- α_1 = sticking coefficient
 b = grain boundary thickness
 C_o = equilibrium solubility of the solid in the liquid
 d_1 = density of solid phase
 D = diffusion coefficient of the slowest moving species
 D_g = grain boundary diffusion coefficient
 D_S = surface diffusion coefficient
 D_V = volume diffusion coefficient
 δ = thickness of liquid film separating the particles
 δ_o = vacancy volume
 δ_{ℓ} = interatomic distance
 η = viscosity
 δ_{LV} = interfacial energy (liquid vapor)
 γ_{SL} = interfacial energy (solid-liquid)
 γ_{SV} = interfacial energy (solid-vapor)
 K = constant
 M = molecular weight
 P_o = equilibrium vapor pressure over a flat surface
 R = gas constant
 T = absolute temperature

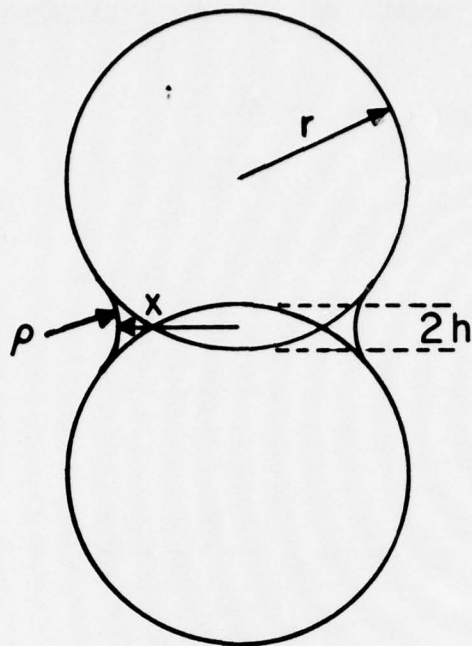


Figure 1. Neck growth during initial stage sintering.

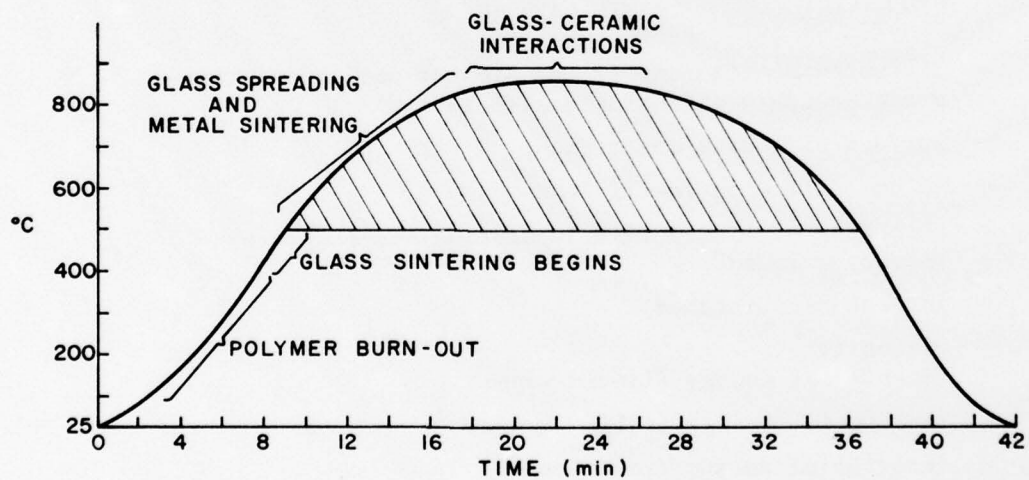


Figure 2. Typical metallization firing profile.

lower temperature the smaller particles begin to densify. As the temperature continues to rise, glass spreading occurs while sintering of the metal constituents proceeds. The Drakenfeld E1527 glass used in the model ink work of the contract series has a softening point of 485°C, i.e., the temperature at which the viscosity is $10^{7.6}$ P. Glass spreading is not considered a major factor until the softening point is exceeded. Above 500°C glass viscosity continues to decrease, and this requires consideration of the possibility of liquid-phase sintering.

All of the metals examined have shown some solubility in E1527 glass [2,3]. Liquid-phase sintering has been reviewed by Eremenko [4], and Fig. 3 illustrates the three stages. The stages are (a) liquid flow or rearrangement of particles to achieve maximum packing efficiency, (b) solution-precipitation, in which portions of the solid phase are dissolved in the liquid phase at areas of high chemical activity and are transported to areas of lower activity where precipitation occurs, and (c) solid-state sintering in which pore closure is completed by solid-state processes, e.g., diffusion by surface, grain boundary, and bulk lattice paths.

The volume of pores initially present in a compacted powder of course varies with particle shape and size distribution. For spherical particles, Kingery's [5] calculations show that a minimum of 35 vol pct of liquid is needed to fill the pores. Under these conditions, rearrangement processes alone can account for complete densification, as shown in Fig. 4. If the liquid volume is less than 35 vol pct, other processes are necessary to densify the compact. Eremenko's review [4] suggests that at least 5 vol pct of liquid is needed to facilitate solution-precipitation.

For systems where the solid is insoluble in the liquid phase, Huppmann [6] has shown that the forces governing particle approach are a function of

2. T. T. Hitch and K. R. Bube, "Basic Adhesion Mechanisms in Thick and Thin Films," Final Report, NASC Contract No. N00019-75-C-0145, 30 Jan. 1976.
3. K. R. Bube and T. T. Hitch, "Basic Adhesion Mechanisms in Thick and Thin Films," Final Report, NASC Contract No. N00019-76-C-0256, 31 Jan. 1977.
4. V. N. Eremenko et al., Liquid-Phase Sintering, Consultants Bureau, New York, 1970, p. 3.
5. W. D. Kingery, "Densification During Sintering in the Presence of a Liquid Phase - I. Theory," J. Appl. Phys. 30, 301 (1959).
6. W. J. Huppmann, "Sintering in the Presence of Liquid Phase," in G. C. Kuczynski, ed., Sintering and Catalysis, Plenum Publishing Co., New York, 1975, p. 359.

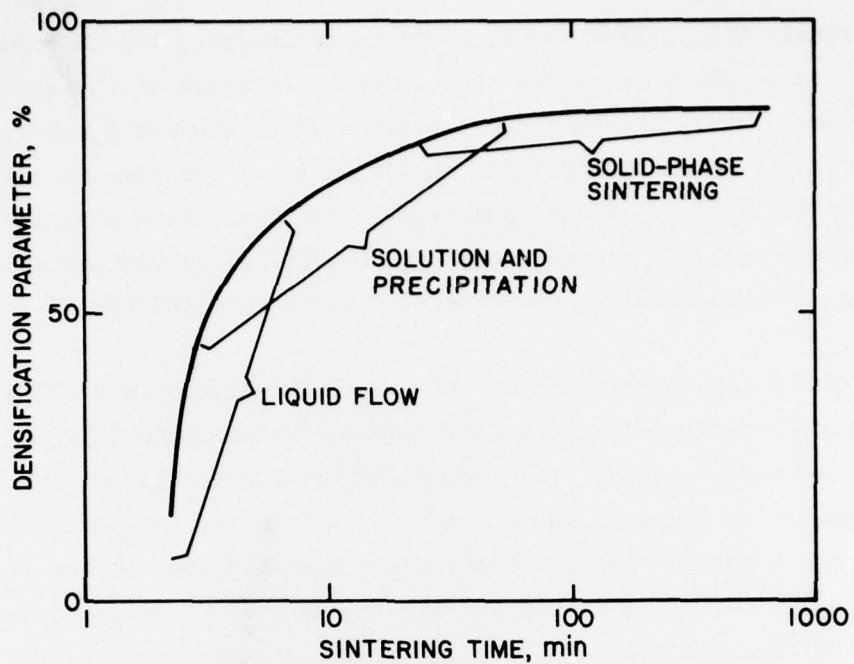


Figure 3. Densification during liquid-phase sintering. After Huppmann [6].

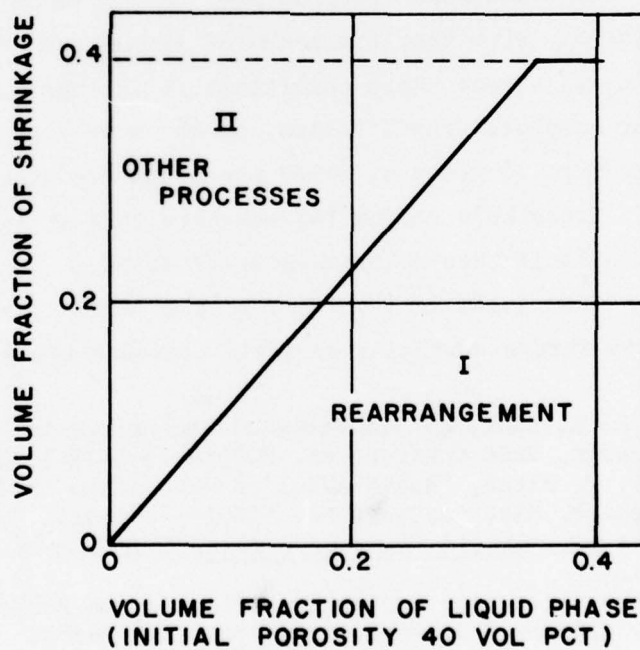


Figure 4. Shrinkage via rearrangement and other processes vs volume fraction of liquid phase. After Kingery [5].

the interfacial energy, γ , between vapor and liquid and the capillary pressure, ΔP , as shown in Fig. 5 and expressed as

$$F = 2\pi r \gamma \cos \phi - \pi r^2 \Delta P \quad (3)$$

where r is the particle radius.

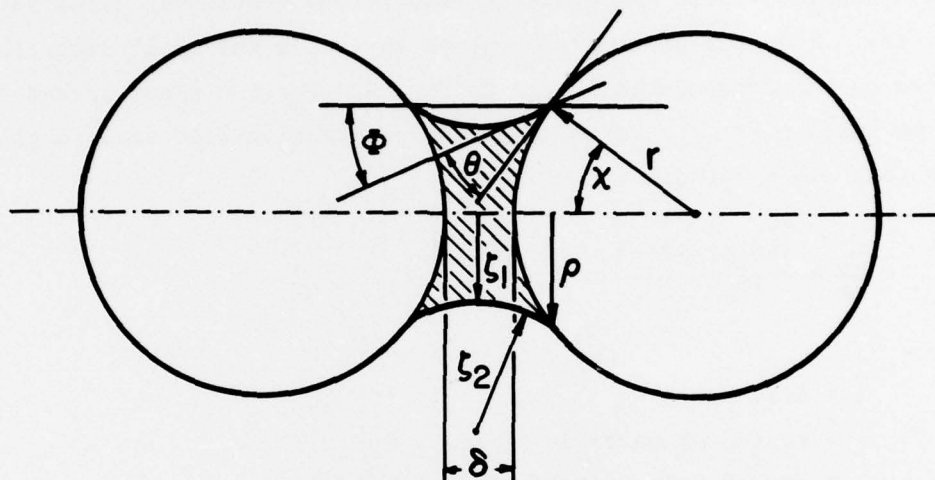


Figure 5. Liquid bridge between particles and resultant force. After Huppmann [6].

Huppmann's calculations and observations show that for systems with good wetting, i.e., $\theta \leq 8^\circ$, a net attractive force increases with increasing volume of the liquid phase. However, as the interparticle distance decreases below $5 \mu\text{m}$, the net attractive force will become progressively greater with lower volume fractions of the liquid.

In our work on gold inks [2,7], advancing contact angle measurements of E1527 on polycrystalline gold were 18.5° , 10° , and 9° , on heating for 10 min to 800°C , 875°C , and 950°C , respectively. These are reasonably close to the 8° angle observed by Huppmann. In addition, the volume fraction of liquid observed by Huppmann was up to 10 vol pct. This value is approximately the same as that

7. T. T. Hitch and K. R. Bube, "Basic Adhesion Mechanisms in Thick and Thin Films," Final Report, NASC Contract No. N00019-C-74-0274, 31 Jan. 1975.

found in thick-film metallizations. Therefore, in the event that the solution-precipitation stage of liquid-phase sintering is not a major contributor to densification in thick-film metallization, the net attractive forces prevalent during the rearrangement stage, as described by Huppmann, will probably provide the greater contribution.

The ability of the glass phase to enhance densification then depends upon the degree to which the glass frit liquefies and spreads over adjacent metal particles. However, while the glass is liquefying, contiguous metal particles are sintering. The dual phenomena of glass spreading and metal sintering are represented by the cross-hatched area in Fig. 2. For the glass spread rate Vest [1] utilized a formula based on liquid penetration into small capillaries and slits [8]. This formula is

$$\frac{dL}{dt} = \frac{r \gamma_{LV} \cos \theta}{4\eta L} \quad (4)$$

where

- L = distance
- r = radius of particle
- γ_{LV} = liquid-vapor interfacial energy
- θ = contact angle between glass and solid
- η = viscosity of the glass

Since the spread rate is proportional to the ratio γ_{LV}/η , the penetration between solid particles depends upon the change of these material properties with temperature. The ultimate microstructure then is the result of two simultaneously occurring phenomena. Thus, variations in microstructure can be achieved through changes in the heating rate, the maximum temperature, the time at peak temperature, and material properties. The critical material properties are metal and glass particle sizes and the γ_{LV}/η ratio vs temperature.

Early sintering studies [2,3] suggested that the powders used were inappropriate for definitive modeling of sintering phenomena. The fine-particle-sized MB-1 mixed-sphere and platelet gold powder sintered extremely rapidly, i.e., at 500°C before glass spreading could occur. Isothermal (900°C) shrinkage curves indicated that powder compact swelling occurred with glass present

8. S. Newman, "Kinetics of Wetting of Surfaces by Polymers; Capillary Flow," J. Colloid Interface Sci. 26, 209 (1968).

at extended firing times [2]. Since the times involved were greater than 5 min and most of the shrinkage had already occurred, the swelling was assumed to be in the terminal stage of sintering. The glass effectively retarded pore closure and contributed to expansion of these pores. The volatilization of PbO trapped in the glass may possibly account for this effect. Since the surface of the powder compact was essentially sealed by sintering at much lower temperatures during heating to 900°C, the subsurface glass, which began to volatilize PbO at 900°C, had no means of escape. This resulted in a pressure buildup in the remaining pores, which was relieved by expansion of the compact at 900°C. However, since the vapor pressure of PbO is only 1 mm of mercury at 943°C [9], this may not be a major factor.

Alternatively, the glass could have contributed to the entrapment of any air that was present in the compact prior to sintering. When the compact was heated, the channels and pores, which were normally open to the surface, were blocked by molten glass. The trapped air created a pressure greater than that derived from the normal sintering forces, i.e., negative capillary pressure [1],

$$\Delta P_p = \frac{-2\gamma_{LV}}{r_p} \quad (4)$$

where r_p = pore radius. This negative pore pressure increased as the pore size decreased, leading to a greater driving force for pore closure. However, if a sufficient quantity of a gas (e.g., air) that is insoluble in either the solid or liquid is present in the pore, the pressure buildup on heating may exceed the negative capillary pressure and cause pore expansion rather than contraction.

The sintering results with the second powder studied, MJ-2, which was all spherical and larger in particle size, tend to confirm the latter alternative. Swelling, after initial sintering, was observed when no glass was present [2]. In this case only trapped air or reducing agent, absorbed during powder precipitation, can account for the swelling. In either powder, the degree of compaction used in making the powder compact may actually contribute to sealing in air before sintering. Therefore, excessive pressure during compaction may hinder ultimate densification.

9. Handbook of Chemistry and Physics, 48th ed., The Chemical Rubber Co., Cleveland, Ohio, 1967, p. D-115.

When glass was added to MJ-2 powder and sintering carried out at 900°C, the shrinkage improved dramatically, in apparent agreement with liquid-phase sintering theory [2]. In order to develop a useful model for microstructure formation in thick-film metallization, more definitive experiments need to be conducted. By holding the glass composition and material properties constant and by varying metal powder morphology, one can clarify the role, if any, of liquid-phase sintering in thick-film metallization. This may be accomplished by a series of isothermal sintering studies, at temperatures that encompass those experienced in a normal firing process, e.g., those below, at, and above the temperature where glass spreading and metal sintering begin, as shown in Fig. 2.

B. POWDER PREPARATION

It was desired to make gold powders with controlled particle size. In the initial work, Au was precipitated from AuCl_3 solution, as described below. The Au was dissolved in aqua regia, and the pH adjusted to 2.5 by addition of NaOH. The solution was kept below 50°C during this period and cooled to room temperature prior to the addition of Na_2SO_3 solution. The specific amounts involved were:

Au	19.9 g
37% HCl	30 ml
70% HNO_3	85 ml
50% NaOH	48 ml
Na_2SO_3	25 g in 175 ml of water

The Na_2SO_3 solution was added with stirring in about 30 s. The precipitated gold was rinsed in deionized water and oven-dried for 40 min at 70-95°C, followed by 30 min at 95-125°C. The yield was 98 wt pct.

Figure 6 illustrates the as-precipitated particle size. This powder, designated MK-2, is generally spherical in shape and larger than MB-1. Because of the larger particle size, MK-2 did not sinter as rapidly as MB-1. The microstructure in Fig. 7 shows some neck growth, but considerable porosity remains.

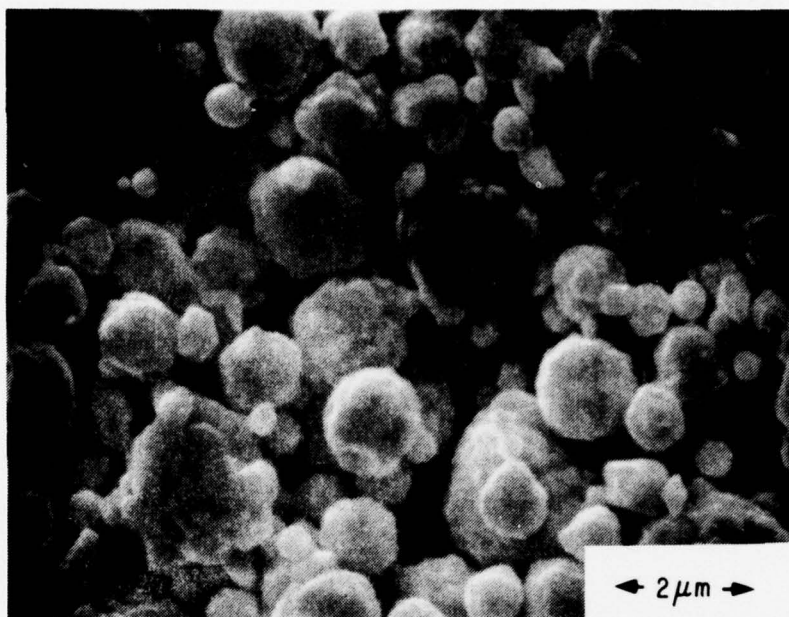


Figure 6. MK-2 gold powder - as precipitated.

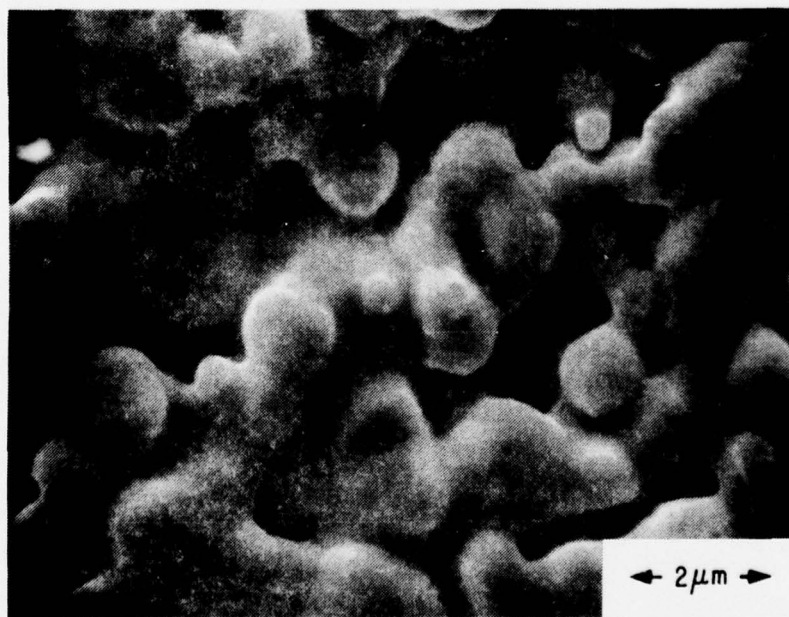


Figure 7. MK-2 gold powder - sintered at 500°C for 2 min.

C. ISOTHERMAL SHRINKAGE

The MK-2 powder was compacted in a 0.5-in. (12.5-mm)-diameter carbide die at 1900-lb (864 kg) pressure and heated for 2, 20, and 300 min at 900°C. Additional samples were prepared with 10 vol pct El527 frit and fired under the same conditions as the pure metal compacts. Figure 8 and 9 show the shrinkage vs time for the pure metal and the metal plus 10 vol pct glass, respectively. The newly precipitated powder, MK-2, exhibits a shrinkage behavior similar to that of the commercially available MJ-2 powder. If glass is not present, both the MJ-2 and MK-2 show rapid initial sintering, followed immediately by swelling (Fig. 8). When glass is added, both powders show considerable improvement in densification (Fig. 9). In contrast, the fine-particle MB-1 gold densifies less with, than without, the glass present.

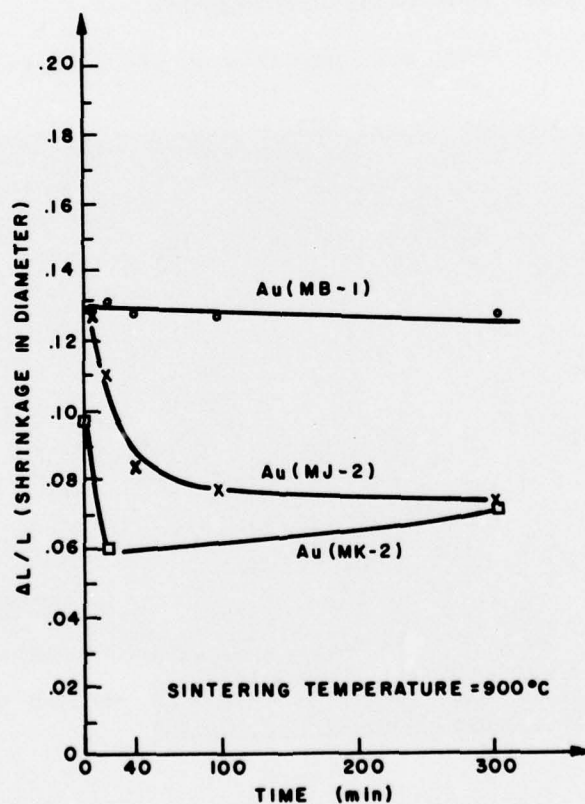


Figure 8. Shrinkage of gold powders at 900°C.

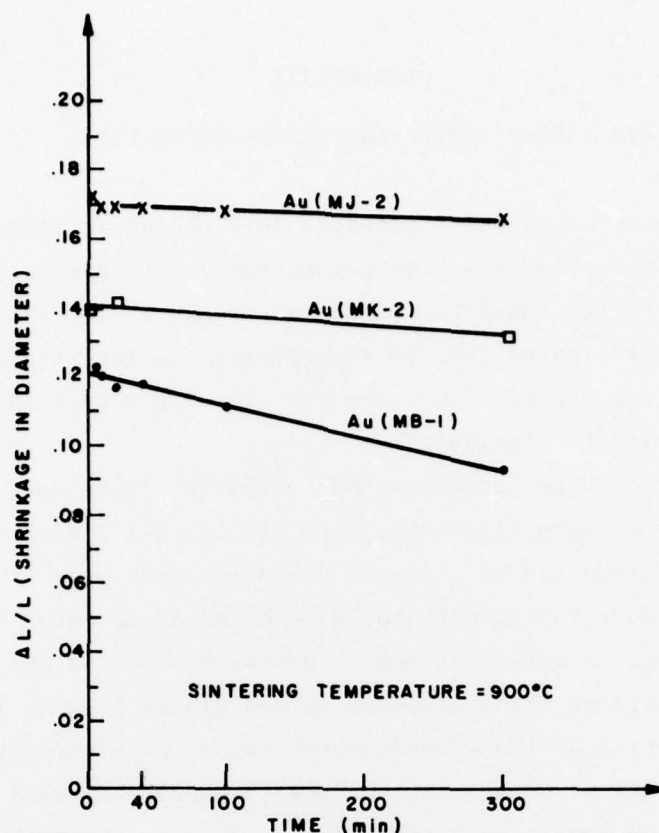


Figure 9. Shrinkage of gold powders plus 10 vol pct E1527 glass at 900°C.

If the metal particle size is large enough, liquid-phase-assisted re-arrangement (first-stage sintering) appears to occur with the glass selected for this study. This does not necessarily imply that solution-precipitation (second stage) processes are involved. Further isothermal sintering studies need to be conducted to clarify this point. Also, microstructure analyses must be undertaken to confirm densification improvements and enhanced grain growth.

SECTION III

REACTIVELY BONDED AND MIXED-BONDED FILMS

The investigation of adhesion strength development in inks containing copper in their binder phase has been concentrated throughout the contract series on identifying the character of the materials at the metal-ceramic interface. It is anticipated that by identifying the interfacial structure, the mechanism by which the adhesion strength of noble metals to the binder phase is enhanced will be elucidated.

In the earlier contract studies three techniques were used to study these materials: low-angle electron diffraction, Auger electron spectrometry, and SEM. All were performed on surfaces which had been mercury-vapor-leached and vacuum-baked. No crystallinity could be detected by means of low-angle electron diffraction. Auger spectrometry was successful in determining the concentrations of binding phase elements in the binder layers, in making a first-order correlation of the adhesion with copper concentration, and in profiling the binder element concentrations versus depth. Results obtained with SEM indicated that no appreciable part of the adhesion strength of these materials could be attributed to a physical interlocking of the metal and the binder phases. SEM also made it possible to observe the formation of a crystalline phase (or phases) in the interface between the metal phase and the alumina substrate. This quarter an investigation was undertaken to identify the crystalline phases at the interface.

One of the most powerful techniques for the identification of crystal phases is x-ray diffraction by means of a powdered sample and use of the Debye-Scherrer camera method. To obtain a sufficient quantity of sample for the test, 1-in. x 1-in. x 0.025-in. substrates were printed with ink over a $(3/4\text{-in.})^2$ area, dried, and fired at temperatures which had produced high adhesion strength. The metal phase was leached away by mercury vapor and the surface scraped with a polycrystalline diamond tool (Megadiamond Industries, NYC, No. SP-10).

The scrapings were collected and studied by x-ray diffraction. The x-ray source was copper with a nickel filter (i.e., Cu $K\alpha$ radiation was used).

Some chipping of the diamond tool was evident, due, in part, to the tool holder design. Because of this, control samples were prepared of the diamond tool chips as well as from scrapings of as-received substrates from the two lots on which thick films had been prepared for the study.

The results are shown in Table 3. The carbon and silicon carbide lines are attributed to the scraper and may be disregarded. A comparison of the data for each sample with that for the appropriate control substrate gives a clear indication that changes in the surface crystallinity were caused by the thick-film bonding agents present in several of the samples. For gold ink H-1, the amount of sample studied was apparently too small to obtain a good pattern. This material will be rerun with powders collected from a larger printed area. In silver ink B-3 the detection of a spinel phase, not seen in an equally strong pattern from the substrate, is taken as an indication of the importance of the spinel phase to the high adhesion strength in this material. In the extremely high adhesion silver ink C-7 fired onto substrate D, the spinel phase was more prominent than in the sample from silver ink B-3.

In the control sample of substrate A, a very weak spinel-phase pattern was detected and *high cordierite* was detected more strongly. In silver ink C-7 fired on substrate A, the intensities from high cordierite and the spinel are reversed, suggesting the possible transformation of some of the high cordierite components into spinel.

It will be noted in Table 3 that the spinels CuAl_2O_4 and MgAl_2O_4 are shown together. These two materials are isomorphic, and their lattice spacing is so nearly the same that it is difficult to determine which one is present, since only medium-to-weak front reflection lines were found. Some differences in intensity between the lines for these two compounds are indicated by the ASTM card file of x-ray diffraction data. These result from the differences in the atomic scattering factors of the copper and magnesium occupying the same spinel lattice sites. However, we could not clearly distinguish between the spinel phases in these three samples. It is believed that the spinel is not pure and is of the mixed form $\text{Cu}_x\text{Mg}_{1-x}\text{Al}_2\text{O}_4$. A copper-containing aluminum silicon oxide similar to $\text{Mg}_2\text{Al}_4\text{Si}_5\text{O}_{18}$ was searched for, but is not listed in the ASTM card file.

All the data found are shown in Table 3: no lines remained unaccounted for. The patterns of the two forms of copper aluminum oxide, CuAlO_2 , were

TABLE 3. PHASE IDENTIFICATION BY X-RAY POWDER DIFFRACTION

Sample Description				x-Ray Data								
Ink Type	Bond	Substrate*	Firing Temperature (°C)	Peel Adhesion Strength (g)	Color of Scraped Area	New Crystal-line Phase Seen in SEM	General Intensity of Patterns on a Film	Relative Strength of Phase Patterns Within a Film				Silicon Carbide
								α -Al ₂ O ₃	Mg ₂ Al ₄ Si ₅ O ₁₈	CuAl ₂ O ₄ and MgAl ₂ O ₄	Carbon SiC	
Au H-1	reactive	A (96% Al ₂ O ₃)	1030	~225	light tan	believed seen	weak	medium	-	-	medium	very weak
Ag B-3	mixed	D (99.5% Al ₂ O ₃)	950	~270	brown	seen	strong	strong	-	very weak	very weak	-
Ag C-7	mixed	D	950	>370	grey	prominent	strong	strong	-	weak	very weak	-
Ag C-7	mixed	A	950	~300	grey-green	unsure	medium	strong	very weak	medium	-	-
		** A			white		strong	strong	very weak	-	very weak	-
		** D			white		strong	strong	weak	very weak	-	-
		diamond + fragments					weak	-	-	-	strong	weak

*Unless otherwise indicated.

**Control sample (as-received substrate).

†Control sample from scraper material.

searched for specifically, but very strong lines of alumina would be superimposed on the strongest lines of one of the forms of this compound, if it were present. Thus, the presence of that form cannot be ruled out completely; the other form of CuAlO_2 , however, was clearly not present.

The indications which may be drawn from the scraping and x-ray-diffraction work are more meaningful when considered in the light of several related papers found in the literature. The $\text{CuO-Al}_2\text{O}_3$ phase diagram has been studied over the composition range of principal interest, and shows that only CuAlO_2 may be expected as a product of the reaction of CuO and Al_2O_3 above a temperature of 1100°C . Between 800 and 900°C , CuAl_2O_4 is the only expected product [10]. Between 900 and 1000°C both CuAl_2O_4 and CuAlO_2 are found. Of course, the presence of an isomorphic spinel of very similar lattice size, e.g., MgAl_2O_4 , and the depletion of oxygen under a sintering metal film are expected to influence the equilibrium between CuO , Al_2O_3 , and their products.

At RCA, mixtures of copper oxide with both pure alumina powder and ground 96-wt pct alumina (substrate A) were fired for 1 h at 1075°C . Copper aluminate spinel CuAl_2O_4 and CuAlO_2 were formed in both cases, but from the alumina ground from the substrate, the CuAlO_2 appeared to form preferentially [2]. Loasby [11] has noted the importance of CuAlO_2 at the interface in thick-film conductors with improved adhesion strength. Burgess and Neugebauer [12] note the possibility of an intermediate phase present aiding the bonding of metal layers to alumina, but indicate their belief that a very close contact between the metal film and the substrate is largely responsible for the adhesion strength of their system. They only admit to the possibility of an intermediate layer a few molecules thick between the copper and the alumina. A mercury-vapor leach, scrape, and x-ray analysis of their oxygen-copper eutectic bonded copper film would be instructive.

10. S. K. Misra and A. C. D. Chaklader, "The System Copper Oxide Alumina," J. Am. Cer. Soc. 46, 509 (1963).
11. R. G. Loasby, N. Davey, and H. Barlow, "Enhanced Property Thick-Film Conductor Pastes," Solid-State Technology 15(5), 46 (1972).
12. J. F. Burgess and C. A. Neugebauer, "The Direct Bonding of Metals to Ceramics and Application in Electronics," Electrocomponent Sci. Technology 2, 233 (1976).

In an excellent paper, Katz [13] has discussed intermediate layers in systems of metal on ceramic and has demonstrated extremely high adhesion strengths in a copper film evaporated onto both polycrystalline alumina and sapphire substrates; these substrates had previously been coated with copper by evaporation and the copper had been oxidized at 1090°C for 66 h. Using x-ray diffraction on the oxidized binder layer, Katz showed CuAl_2O_4 to have been the primary binder phase. The precoated substrates were rust-colored and appeared frosted on the polished sapphire substrates.

In the study of both the mixed-bonded and reactively bonded conductors, a major question is, "How do the binder agents move to the metal film-substrate interface?" The high solubility of copper oxide in the lead oxide glass E1527 has been demonstrated at RCA [2]. Similar to the mechanism described in the comments on liquid-phase sintering, solution of the copper oxide into, and precipitation from, the molten frit is taken to be a highly likely transport mechanism. By this mechanism the kinetics of adhesion strength development in mixed-bonded inks can be understood to be faster than those of reactively bonded inks.

13. G. Katz, "Adhesion of Copper Films to Aluminum Oxide Using a Spinel Structure Interface," *Thin Solid Films* 33, 99 (1976).

SECTION IV

FUTURE WORK

Many factors could be important to the microstructural development and, hence, to the adhesion strength of frit-bonded thick films. Some of these are:

Print thickness; ink-vehicle evaporation and burnoff; metal particle size and shape distribution; bulk-metal surface free energy; metal purity; frit particle size and shape distribution; temperature influence on frit viscosity; wetting angle of frit on the metal and on the ceramic substrate; solubility of substrate in molten frit as a function of temperature and time; sintering characteristics of the metal; devitrification of frit as a function of temperature, time, and dissolved substrate in the frit; penetration of frit into the substrate surface; metal-to-frit volume ratio; glass flow in the sintering-metal microstructure; and thermal history.

In the coming quarter RCA must continue with the identification of those factors which are critically important and will begin to construct a model of microstructure development in frit-bonded conductors.

Work is planned on several items important to the experimental phase of the study. A quantity of gold powder will be produced by chemical precipitation and used in isothermal shrinkage studies at several temperatures from 400 to 900°C. Microstructural analysis will be used to determine if grain growth is enhanced in the presence of glass. Variations in compaction pressure may be tried as a means of eliminating the swelling, described earlier, which occurs when these gold powders are sintered at high temperatures.

In the study of copper-containing binders and adhesion strength development, further work is required on the kinetics of binder phase formation as well as on the identification of important binder phases. Along with other studies of these phenomena, x-ray diffraction of powder samples is planned.

A review of the pertinent available ceramic phase diagrams will be made. This will be supplemented by a study of the glass systems pertinent to thick-film binders, which has been undertaken at Purdue University. These studies should lead to a better understanding of frit-bonded and mixed-bonded conductors, as well as of reactively bonded conductors.

Work at NRL on reactively bonded inks is also expected to help us understand these materials. NRL has unique capabilities for several analytical methods; the results of studies now underway in which these methods are employed should be invaluable in the modeling of adhesion development in reactively bonded inks.

REFERENCES

1. R. W. Vest, "Conduction Mechanisms in Thick-Film Microcircuits," Final Technical Report under ARPA Order No. 1642, Grant Nos. DAHC-15-70-G7 and DAHC-15-73-G8. Grantee: Purdue Research Foundation, Dec. 1975.
2. T. T. Hitch and K. R. Bube, "Basic Adhesion Mechanisms in Thick and Thin Films," Final Report, NASC Contract No. N00019-75-C-0145, 30 Jan. 1976.
3. K. R. Bube and T. T. Hitch, "Basic Adhesion Mechanisms in Thick and Thin Films," Final Report, NASC Contract No. N00019-76-C-0256, 31 Jan. 1977.
4. V. N. Eremenko et al., Liquid-Phase Sintering, Consultants Bureau, New York, 1970, p. 3.
5. W. D. Kingery, "Densification During Sintering in the Presence of a Liquid Phase - I. Theory," J. Appl. Phys. 30, 301 (1969).
6. W. J. Huppmann, "Sintering in the Presence of Liquid Phase," in G. C. Kuczynski, ed., Sintering and Catalysis, Plenum Publishing Co., New York, 1975, p. 359.
7. T. T. Hitch and K. R. Bube, "Basic Adhesion Mechanisms in Thick and Thin Films," Final Report, NASC Contract No. N00019-C-74-0270, 31 Jan. 1975.
8. S. Newman, "Kinetics of Wetting of Surfaces by Polymers; Capillary Flow," J. Colloid Interface Sci. 26, 209 (1968).
9. Handbook of Chemistry and Physics, 48th ed., The Chemical Rubber Co., Cleveland, Ohio, 1967, p. D-115.
10. S. K. Misra and A. C. D. Chaklader, "The System Copper Oxide Alumina," J. Am. Cer. Soc. 46, 509 (1963).
11. R. G. Loasby, N. Davey, and H. Barlow, "Enhanced Property Thick-Film Conductor Pastes," Solid-State Technology 15(5), 46 (1972).
12. J. F. Burgess and C. A. Neugebauer, "The Direct Bonding of Metals to Ceramics and Application in Electronics," Electrocomponent Sci. Technology 2, 233 (1976).
13. G. Katz, "Adhesion of Copper Films to Aluminum Oxide Using a Spinel Structure Interface," Thin Solid Films 33, 99 (1976).